A Biphenyl Type Two-Photon Fluorescence Probe for Monitoring the Mitochondrial Membrane Potential

H. Moritomo[1], K. Yamada[2], Y. Kojima[3], Y. Suzuki[1,3], S. Tani[2,3], H. Kinoshita[4], A. Sasaki[5], S. Mikuni[4], M. Kinjo[4], J. Kawamata[1,3,*]

Graduate Schools of [1]Medicine, [2]Science and Engineering, and [3]Department of Chemistry, Faculty of Science, Yamaguchi University, Yamaguchi, Japan

[4]Laboratory of Molecular Cell Dynamics, Faculty of Advanced Life Science, Hokkaido University, Sapporo, Japan

[5]Laboratory for Nano-Bio Probes, Quantitative Biology Center, Osaka, Japan

Running title: A novel two-photon fluorescence probe

[*]Correspondence to: J. Kawamata

Graduate School of Medicine, Yamaguchi University

Yoshida, Yamaguchi 753-8512, Japan

Tel/Fax: +81 83 933 5729

E-mail: j_kawa@yamaguchi-u.ac.jp

Abstract

Here we describe the design and synthesis of a bifunctional two-photon fluorescence probe, *N*,*N*'-dimethyl-4,4'-(biphenyl-2,1-ethenediyl)dipyridinium hexafluorophosphate (BP6). HeLa, Hek293, and *Paramecium caudatum* cells were stained with BP6. BP6 accumulated on the mitochondria of all three cell types when the mitochondrial membrane potential was high. As the mitochondrial membrane potential decreased following the addition of carbonyl cyanide *m*-chlorophenyl hydrazine, BP6 moved from the mitochondria to the nucleus in a reversible manner, depending on the mitochondrial membrane potential status. The maximum value of the two-photon absorption cross-section of BP6 is 250 GM (1 GM = 1×10^{-50} cm^4 s $molecules^{-1}$ $photon^{-1}$). This value is 3 and 30 times larger, respectively, than that of the conventional mitochondria selective probes, rhodamine 123 and green fluorescence protein. These results suggest that BP6 should be useful for monitoring mitochondrial membrane potential by two-photon excitation.

Key words: Two-photon fluorescence, fluorescence probe, mitochondrial membrane

potential, biphenyl derivative

Introduction

Monitoring mitochondrial membrane potential is useful for understanding cell activity. When cell activity decreases, the mitochondrial membrane potential also decreases (Savitskiy *et al*., 2003; Ly *et al*., 2003). Therefore, fluorescent probes which are responsive to mitochondrial membrane potential enable active cells to be discriminated from less active cells (Russel *et al*., 1999). Development of an efficient two-photon absorption probe sensitive to mitochondrial membrane potential might allow three-dimensional imaging of the activity of individual cells in body organs by two-photon fluorescence microscopy (Denk *et al*., 1990).

We previously reported an efficient two-photon fluorescence mitochondrial selective probe, 1,1'-diethyl-4,4'-(9,9'-diethyl-2,7-fluorenediyl-2,1-ethanediyl)dipyridinium perchlorate (FLW; Fig. 1(a)). The maximum value of the two-photon absorption cross-section ($\sigma^{(2)}$, which indicates the efficiency of two-photon absorption, of FLW was 730 GM (1 GM = 1×10^{-50} cm^4 s molecules^{-1} photon^{-1}) at 750 nm (Tani *et al*., 2012). This value is 9 and 90 times larger than that of the typical mitochondrial selective probes, rhodamine 123

(Wolleschensky *et al*., 1998) and green fluorescent protein (GFP) (So *et al*., 2000), respectively. FLW comprises a highly fluorescent fluorene core and cationic pyridinium groups connected by vinylene groups. Due to the cationic pyridinium group, FLW exhibits high water solubility and accumulates on the mitochondria through electrostatic interactions with the negatively charged mitochondrial inner membrane (Tani *et al*., 2012).

A mitochondrial membrane potential sensitive probe, 4-(2-(6-(dibutylamino)-2-naphthalenyl)ethenyl)-1-(3-sulfopropyl)pyridinium (di-4-ANEPPS) (Novakova *et al*., 2008), is structurally similar to FLW. Specifically, the aromatic ring and pyridinium group of di-4-ANEPPS are connected by a vinylene group. Although the presence of a vinylene group is reported to be essential for monitoring membrane potential by di-4-ANEPPS, FLW is unresponsive to mitochondrial membrane potential. It has been pointed out that cationic compounds with a large polarizability tend to bind strongly to the mitochondrial membrane (Rosania *et al*., 2003). Since FLW has a large and planar π-conjugated system with a strong electron-acceptor moiety, its polarizability should be very large. Therefore, FLW is

thought to bind strongly with the mitochondrial membrane and thus is not responsive to mitochondrial membrane potential.

In this study, we aimed to create a novel two-photon fluorescence probe that exhibits mitochondrial membrane potential sensitivity. We have designed and synthesized a molecule that is structurally similar to FLW but exhibits smaller polarizability: *N*,*N*'-dimethyl-4,4'-(biphenyl-2,1-ethenediyl)-dipyridinium hexafluorophosphate (BP6; Fig. 1(b)). In order to decrease polarizability, the central part of the structure was changed from a planar fluorene to a twisted biphenyl. This change in molecular structure was predicted to introduce a twisted π-electron system into BP6. The twisted π-electron system of BP6 should prevent delocalization of the π-electrons over the entire molecule, resulting in low polarizability. At high mitochondrial membrane potential, BP6 localized on the mitochondria. When the mitochondrial membrane potential became low, BP6 moved from the mitochondria to the nucleus. It is known that a smaller polarizability induces a smaller $\sigma^{(2)}$ (He *et al*., 2008). Therefore, the $\sigma^{(2)}$ of BP6 was smaller than that of FLW, but was larger than that of conventional mitochondrial selective probes. Thus, BP6 balanced the competing

goals of exhibiting efficient two-photon absorption properties and mitochondrial membrane potential sensitivity.

Material and Methods

Synthesis

4,4'-Diformylbiphenyl. 4,4-Dibromobiphenyl (1.56 g, 5 mmol) was dissolved in dry tetrahydrofuran (THF) and stirred at -78°C. *n*-Butyllithium (1.6 mol L^{-1} (M) in hexane, 20 mL) was added dropwise for 1 hour to the solution, and then the solution was stirred for a further 20 minutes. A mixture of dry *N*,*N*-dimethylformamide (5 mL) and dry THF (6 mL) was added to the reaction mixture and the mixture was stirred at ambient temperature for 3 hours. The reaction was quenched by pouring HCl aqueous solution (1 N, 45 mL) into the reaction mixture at -5°C. The reaction mixture was extracted with water and toluene, and then the organic phase was evaporated. The resultant solid was recrystallized from toluene to obtain 4,4'-diformylbiphenyl (44% yield) (^{1}H NMR [400 MHz, $CDCl_3$, ppm], δ=10.02 [s, 2H, formyl], δ=8.04 [d, *J*=8.8 Hz, 4H, phenyl], δ=7.84 [d, *J*=8.4 Hz, 4H, phenyl]).

N,N'-Dimethyl-4,4'-(biphenyl-2,1-ethenedilyl)dipyridinium iodide.

4,4'-Diformylbiphenyl (0.2124 g, 1 mmol) and 1,4-dimethylpyridinium iodide (0.42 g, 2 mmol) were dissolved in a mixture of chloroform (15 mL) and methanol (35 mL). Piperidine was dropped into the reaction mixture and the mixture was stirred for 6 hours at 60°C. The solvent was evaporated and the resultant solid was recrystallized from methanol to obtain *N,N*'-dimethyl-4,4'-(biphenyl-2,1-ethenedilyl)dipyridinium iodide as a yellow solid (52% yield) (^{1}H NMR [400 MHz, dimethyl sulfoxide (DMSO)-d_6, ppm], δ=8.89 [d, *J*=6.4 Hz, 4H, pyridyl], δ=8.25 [d, *J*=6.8 Hz, 4H, pyridyl], δ=8.09 [d, *J*=16 Hz, 2H, ethenyl], δ=7.95 [d, *J*=8.4 Hz, 4H, phenyl], δ=7.89 [d, *J*=8.4 Hz, 4H, phenyl], δ=7.62 [d, *J*=16 Hz, 2H, ethenyl], δ=4.27 [s, 6H, -CH_3]).

N,N'-Dimethyl-4,4'-(biphenyl-2,1-ethenedilyl)dipyridinium hexafluorophosphate (BP6).

N,N'-Dimethyl-4,4'-(biphenyl-2,1-ethenedilyl)dipyridininium iodide (0.65 g, 1 mmol) and sodium hexafluorophosphate (0.84 g, 5 mmol) were dissolved in methanol (20 mL) and stirred overnight. The precipitate was filtered. The residue was recrystallized from methanol to obtain *N,N*'-dimethyl-4,4'-(biphenyl-2,1-ethenedilyl)dipyridinium

hexafluorophosphate (70% yield).

The water solubility of BP6 was on the order of 0.1 mM.

Spectroscopy

One-photon absorption spectra were recorded on a V-670-UV-VIS-NIR spectrophotometer (Jasco Co., Tokyo, Japan). Fluorescence spectra and fluorescence quantum yields were obtained using an absolute photoluminescence quantum yield measurement system (C9920-02G, Hamamatsu Photonics K. K., Hamamatsu, Japan). The fluorescent dyes, Mito Tracker Deep Red 633 (Mito Tracker, Invitrogen, Carlsbad, CA) and JC-1 (Invitrogen) tend to aggregate in water. This prevents reliable evaluation of fluorescence quantum yields. We confirmed that these dyes do not aggregate in DMSO at a low concentration. Therefore, quantum yield measurements were conducted using DMSO as the solvent. Two-photon absorption (TPA) spectra were measured using the open-aperture Z-scan technique (Sheik-Bahae *et al*., 1990). A femtosecond pulsed beam from an optical parametric amplifier (OPA-800C, Spectra-Physics, Santa Clara, CA) pumped by a beam from a regenerative amplifier (Spitfire, Spectra-Physics) was

used as the light source. The typical pulse duration was 150–200 fs and the repetition rate was 1 kHz. The incident beam was focused by a plano-convex lens (f = 150 mm). The sample solution was scanned along the incident beam axis. The average peak power was varied from 0.01 to 0.4 mW, corresponding to on-axis peak powers of 6 to 240 GW/cm^2. The measurements revealed that the two-photon absorbance (q_0) is proportional to the incident power (I_0). This is a reliable indication that the transmittance changes observed from the Z-scan measurements were purely due to TPA and not to any other nonlinear optical process. Reliable Z-scan measurements require that the sample be thinner than the Rayleigh length and contain many dye molecules in the optical path. Thus, the use of a concentrated solution of BP6 will provide accurate results. The solubility of BP6 in DMSO was considerably higher than that in water. Therefore, Z-scan measurements were performed using a DMSO solution of BP6.

Live cells and labeling

Strain RB-1 (mating type E, syngen 4) of *Paramecium caudatum* (*P. caudatum*) was a gift from Prof. M. Fujishima (Graduate School of Science and

Engineering, Yamaguchi University, Japan) and was maintained in rice straw medium. *P. caudatum* was treated with medium containing 500 nM BP6 for 12 hours. To introduce JC-1 into the cells, *P. caudatum* was treated with medium containing 500 nM JC-1 for 15 minutes. HeLa and Hek293 cells were maintained in Dulbecco's modified Eagle's medium (DMEM, Sigma-Aldrich Japan, Shinagawa, Japan) supplemented with penicillin, streptomycin, and 10% (v/v) fetal bovine serum (FBS, Sigma-Aldrich Japan) at 37°C in 5% CO_2. HeLa and Hek293 cells were treated with medium containing 500 nM BP6 for 16 hours. HeLa cells were further treated with 500 nM of Mito Tracker for 30 minutes. HeLa and Hek293 cells were then washed several times with phenol-red-free medium (Opti-MEM, Invitrogen) supplemented with 10% (v/v) FBS.

Microscopy

Single photon fluorescence microscopy (SPFM). Single photon fluorescence microscopy (SPFM) was carried out with an LSM510 (Zeiss, Jena, Germany) equipped with a temperature control system. Cells in a 35 mm glass-base dish were stained with BP6, JC-1 and Mito Tracker. BP6 and JC-1 were then excited using a 405 nm diode

laser, aggregated JC-1 was excited using a 543 nm He-Ne laser, and Mito Tracker was excited using a 633 nm He-Ne laser. All excitations were performed through a water immersion objective (C-Apochromat, 40, 1.2 NA; Zeiss). The emission signals from BP6 and JC-1 were collected by a photomultiplier tube through a 505–550 nm band-pass filter, and the signals from aggregated JC-1 and Mito Tracker were collected at 647–754 nm.

Estimation of the swimming speed of P. caudatum. The swimming speed of *P. caudatum* in medium containing 0, 5, 7.5 or 10 μM carbonyl cyanide *m*-chlorophenylhydrazone (CCCP) was determined by SPFM. The swimming speed was recorded 5 minutes after the addition CCCP, as follows. A fluorescence image was obtained every 0.5 seconds, and the migration distance of *P. caudatum* between each image was estimated. The migration distance was divided by the time difference between each image, thereby allowing the swimming speed to be determined. The reported estimated swimming speed at each CCCP concentration is the average value obtained from 50 *P. caudatum* cells.

Two-photon fluorescence microscopy (TPFM). Two-photon fluorescence microscopy (TPFM) was carried out using a Ti:sapphire femtosecond laser (Mira, Coherent, Santa Clara, CA) as the light source. A galvano scanner (C10516, Hamamatsu Photonics K. K.) was used as the laser scanning unit. Cells were placed in a 35 mm glass-base dish. The sample was placed on a motor-controlled z-stage, excited by a 750 nm femtosecond laser through a water immersion objective (UApo 340 40X, OLYMPUS, Tokyo, Japan), and scanned along the optical axis. A photomultiplier tube (R212, Hamamatsu Photonics K. K.) was used for signal detection.

Computational methods

The molecular structures of BP6, FLW, and di-4-ANEPPS were optimized using density functional theory (DFT) in Gaussian 03 (Gaussian Inc., Wallingford, CT), employing Becke's three-parameter exchange (Becke 1993), the Lee, Yang, and Parr correlation (B3LYP) hybrid functional (Lee *et al*., 1988), and the 6-31+G** basis set (Rassolv *et al*., 1998). The polarizabilities were calculated at the same level of theory as

for the geometry optimizations. All calculations were carried out *in vacuo*.

Results and Discussion

The absorption and fluorescence spectra of an aqueous solution of BP6 are shown in Fig. 2. The spectroscopic data and polarizability estimated by DFT calculation of BP6 are summarized in Table I, together with the values for FLW. The absorption maximum (λ_{abs}) and fluorescence maximum (λ_{fl}) wavelengths of BP6 were 384 and 527 nm, respectively. These values were blue-shifted 34 and 26 nm compared to those of FLW. It is well known that the smaller the π-conjugated system, the shorter the wavelength of the absorption and fluorescence maxima. Therefore, these shorter wavelengths are attributed to division of the π-conjugated system caused by the decreased planarity of the central part of the molecule. Thus, the polarizability of BP6 should be decreased compared to that of FLW. In fact, the polarizabilities of BP6 and FLW estimated by DFT calculations were 5.61×10^{-29} and 6.40×10^{-29} m^3, respectively, which are much larger than the polarizability of di-4-ANEPP, 2.34×10^{-29} m^3.

The fluorescence quantum yields (ϕ) of rhodamine 123, Mito Tracker, JC-1 and BP6 in DMSO were 0.80, 0.71, 0.051 and 0.40, respectively. Clearly, the fluorescence quantum yield of BP6 is higher than that of JC-1, a typical dye used to monitor mitochondrial membrane potential by SPFM.

Figure 3 shows SPFM images of HeLa, *P. caudatum* and Hek293 cells stained with BP6 and/or Mito Tracker. Figs. 3 (a) and (b) show images of HeLa cells treated with BP6 and Mito Tracker, respectively. The merged image (Fig. 3(c)) revealed that the structure stained with BP6 was very similar to that stained with Mito Tracker; thus, BP6 was judged to accumulate on the mitochondria in HeLa cells.

The division of HeLa cells stained with BP6 was monitored for over 24 hours. No anomalous cell division was observed, indicating that the toxicity of BP6 is sufficiently low to allow its use as a fluorescence probe for live cell imaging.

An SPFM image of *P. caudatum* stained with BP6 is shown in Fig. 3 (f). The bright fluorescence aggregations are likely phagosomes, as reported for cells stained with FLW (Tani *et al*., 2012). Images of mitochondria are shown in the inset and clearly indicate the accumulation of BP6 on the mitochondria of *P. caudatum*. An SPFM image

of Hek293 cells stained with BP6 is shown in Fig. 3 (h) and also shows an accumulation of BP6 on the mitochondria.

The responsiveness of BP6 to mitochondrial membrane potential can be seen from a comparison of Figs. 3 (a), (d), and (e). Figs. 3 (d) and (e) are images of HeLa cells after adding and after removing CCCP, respectively. It is well known that CCCP depolarizes mitochondria by increasing their permeability to protons, causing the collapse of the mitochondrial membrane potential. Fig. 3 (d) indicates that mitochondrial fluorescence disappeared following the addition of CCCP and was replaced with fluorescence from the nucleus, indicating that the BP6 moved from the mitochondria to the nucleus under conditions of low mitochondrial membrane potential. Fluorescence from BP6 was observed from the mitochondria again after the removal of CCCP from the medium (Fig. 3 (e)). This ability to switch which organelle BP6 accumulated on was observed in all three cell types investigated in this study. The switching behavior can be seen from comparison of Figs. 3 (f) and (g) for *P. caudatum*. In Fig. 3 (g), the highest intensity of fluorescence is observed in the nucleus in the center of the cell, while significant fluorescence is also observed from the phagosomes.

Fig. 3 (g) shows higher fluorescence intensity in the nucleus and lower fluorescence intensity in the mitochondria compared to Fig. 3 (f), indicating that the location of PB6 could also be switched in *P. caudatum* cells. Similar switching can also be seen from comparison of Figs. 3 (h) and (i) for Hek293 cells.

The probable mechanism underlying this switching is as follows. Prior to the addition of CCCP, the mitochondria in a cell have a larger negative charge than the nuclei due to the electrochemical proton gradient across the mitochondrial membrane, so BP6 accumulated more effectively on the mitochondria by electrostatic interaction. The addition of CCCP depolarizes the mitochondrial membrane potential and decreases the negative charge on the mitochondria to the point where the negative charge on the nuclei may be larger than that on the mitochondria, resulting in BP6 accumulating preferentially on the nuclei.

BP6 has a unique characteristic not exhibited by other mitochondrial membrane potential sensitive probes used for TPFM imaging. To date, two types of mitochondrial membrane potential sensitive probes have been conventionally used. One is fluorescence color change probes, such as JC-1, where the color depends on the

mitochondrial membrane potential. The other is fluorescence intensity change probes such as di-4-ANEPPS. Detecting fluorescence color change requires changing the excitation light source and the fluorescence filters. For TPFM imaging, changing the excitation light source is impractical. In contrast, in the case of BP6, a change in membrane potential is detected using the same excitation light source. For fluorescence intensity change probes, photo-bleaching of the probe often prevents reliable detection of the change in fluorescence intensity in both single- and two-photon fluorescence microscopy. Since BP6 can move between two types of organelles, there is no possibility of misinterpreting mitochondrial membrane potential due to photo-bleaching of the probe.

The localization of BP6 was compared with the other mitochondrial probes, Mito Tracker and JC-1, by carrying out time-lapse fluorescence microscopy. Images of Hek293 cells stained with BP6, Mito Tracker or JC-1 before and after the addition of CCCP, and after the removal CCCP, are shown in Fig. 4. It is difficult to wash the cells while maintaining them in the field of view, so the same cells were not necessarily observed throughout the observation period. In the original images (prior to the addition

of CCCP) in Fig. 4, BP6, Mito Tracker and JC-1 all accumulated on the mitochondria. Thirty seconds after adding CCCP, BP6 was still localized on the mitochondria; five minutes after adding CCCP, BP6 had partially translocated to the nucleus, and had completely translocated to the nucleus after 10 minutes. In contrast, fluorescence due to Mito Tracker and JC-1 completely disappeared from the mitochondria and appeared in the cytoplasm within 30 seconds of adding CCCP; no further changes in fluorescence distribution were observed even after 10 minutes. Thus, after adding CCCP, BP6 migrates from the mitochondria much more slowly than Mito Tracker and JC-1. BP6 completely translocated from the nucleus to the mitochondria within 30 seconds of removing CCCP, whereas 20 minutes was require for full recovery of mitochondrial fluorescence with Mito Tracker and JC-1 following removal of CCCP. Thus, BP6 moved more rapidly from the nucleus to the mitochondria than the other probes, but moved slowly from the mitochondria to the nucleus.

The photostabilities of BP6 and Mito Tracker were compared by continuously irradiating DMSO solutions of BP6 and Mito Tracker with 365 nm UV light for 1 hour. The fluorescence quantum yields of both dyes decreased by 20% following UV

irradiation.

The swimming speed of *P. caudatum* was used as an indicator of cell activity related to mitochondrial activity. The relationship between cell activity and which organelle BP6 accumulated in was investigated. A plot of the swimming speed of *P. caudatum*, and of the fluorescence intensity on the mitochondria and on the nucleus versus the CCCP concentration in the medium, is shown in Fig. 5. The swimming speed of *P. caudatum* monotonically decreased as the concentration of CCCP increased. The fluorescence intensity of BP6 from the mitochondria was essentially constant below a CCCP concentration of 5 μM. When the CCCP concentration was above 5 μM, the fluorescence intensity of BP6 from the mitochondria decreased significantly, while the fluorescence intensity of BP6 from the nucleus increased. This result indicated that the organelle to which the dye was distributed switches at low membrane potential, and the switching behavior of BP6 requires a threshold mitochondrial membrane potential, consistent with other mitochondrial membrane potential probes. SPFM images of *P. caudatum* stained with JC-1 with 5 and 7 μM CCCP in the medium are shown in Fig. 6. The fluorescence color of JC-1 is known to change from red to green when the

mitochondrial membrane potential becomes low (Smiley *et al*., 1991). Red fluorescence was observed at a CCCP concentration of 5 μM (Fig. 5(a)), whereas green fluorescence was observed at 7 μM CCCP (Fig. 5(b)). The CCCP concentration required to change the fluorescence color of JC-1 corresponded with the concentration required to switch BP6 fluorescence to the nucleus instead of the mitochondria, indicating that BP6 exhibits similar sensitivity to mitochondrial membrane potential as the commercially available probe, JC-1.

The two-photon absorption spectrum of a DMSO solution of BP6 is shown in Fig. 7. The peak of $\sigma^{(2)}$ of BP6 was 250 GM at 740 nm. This wavelength is almost double the wavelength of the "one-photon" absorption band. This TPA transition reflects well the electronic characteristics of the molecule. BP6 has smaller polarizability than FLW; therefore, the $\sigma^{(2)}$ value of the TPA peak of BP6 (250 GM at 740 nm) is smaller than that of FLW (730 GM at 750 nm). However, this value is still considerably larger than that of mitochondrial selective probes such as rhodamine 123 (80 GM) or GFP (8 GM). Thus, BP6 should prove useful not only as a mitochondrial membrane potential sensitive probe, but also as an efficient mitochondria selective

two-photon fluorescence probe.

The brightness of two-photon excited fluorescence dyes is expressed quantitatively by the value of the two-photon action cross-section ($\sigma^{(2)}\phi$), which is the product of the values of $\sigma^{(2)}$ and ϕ. The values of $\sigma^{(2)}\phi$ of rhodamine 123 and BP6 are 64 GM at 800 nm and 100 GM at 740 nm, respectively. Rhodamine 123 has a higher ϕ value than BP6, but BP6 has a higher $\sigma^{(2)}$ value; therefore, the $\sigma^{(2)}\phi$ value of BP6 is larger than that of rhodamine 123. Therefore, BP6 exhibits higher brightness in TPFM than the bright dye, rhodamine 123.

TPFM images of Hek293 cells before and after the addition of CCCP are shown in Figs. 8 (a) and (b), respectively. Similar to the change observed between Figs. 3 (h) and (i), the organelle in which BP6 accumulated was detected by TPFM. We measured the imaging depth from the surface using a celery fraction as a sample. Both BP6 and rhodamine 123 penetrated 600 μm from the surface of the fraction. Thus, BP6 holds promise as a useful probe for detecting mitochondrial membrane potential by TPFM.

Conclusion

In this study, a biphenyl type two-photon fluorescence probe, BP6, was designed and synthesized. BP6 accumulated on the mitochondria at a high mitochondrial membrane potential, but migrated from the mitochondria to the nucleus when the mitochondrial potential decreased. This ability to move between organelles was reversible. The $\sigma^{(2)}$ and water solubility of BP6 was higher than those of conventional mitochondrial selective probes. Therefore, BP6 is a promising probe for monitoring mitochondrial membrane potential by TPFM.

Acknowledgements

This work was supported by a Grant-in-Aid for Scientific Research (no. 23350068) from the Ministry of Education, Culture, Sports, Science and Technology, Japan. Paramecium strain RB-1 used in this study was provided by Symbiosis Laboratory, Yamaguchi University, with support in part by the National Bio-Resource Project of the Ministry of Education, Culture, Sports, Science and Technology, Japan. We are grateful Prof. S. Yumura of Yamaguchi University for his help with the

time-lapse fluorescence imaging experiment.

References

Becke, A. D. 1988. Density-functional exchange-energy approximation with correct asymptotic behavior. *Phys. Rev. A*, **38**; 3098–3110.

Becke, A. D. 1993. Density-functional thermochemistry. III. The role of exact exchange. *J. Chem. Phys.*, **98**; 5648–5652.

Denk, W., Strickler, J. H., Webb, W. W., 1990. Two-photon laser scanning fluorescence microscopy. *Science*, **248**; 73–76.

He, G. S., Tan, L.-S., Zheng, Q., Prasad, N. Multiphoton absorbing materials: molecular designs, characterizations, and applications. *Chem. Rev.* **108**; 1245–1330.

Lee, C., Yang, W., Parr, R. G., 1988. Development of the Colle-Salvetti correlation-energy formula into a functional of the electron density. *Phys. Rev. B: Condens. Matter Mater. Phys*., **37**; 785–789.

Ly, J. D., Grubb, D. R., Lawen, A., 2003. The mitochondrial membrane potential ($\Delta\psi$m) in apoptosis; an update. *Apoptosis*, **8**; 115–128.

Novakova, M., Bardonova, J., Provaznik, I., Taborska, E., Bochorakova, H., Paulova, H., Horky, D., 2008. Effects of voltage sensitive dye di-4-ANEPPS on guinea pig and rabbit myocardium. *Gen. Physiol. Biophys.*, **27**; 45–54.

Rassolov, V. A., Pople, J. A., Ratner, M. A., Windus, T. L. 1998. 6-31G* basis set for atoms K through Zn. *J. Chem. Phys.*, **109**; 1223–1229.

Rosania, G. R., Lee, J. W., Ding, L., Yoon, H. S., Chang, Y. T. 2003. Combinatorial approach to organelle-targeted fluorescent library based on the styryl scaffold. *J. Am. Chem. Soc.*, **125**; 1130–1131.

Russell, C., Scaduto, Jr., Grotyohann, L. W. 1999. Measurement of mitochondrial membrane potential using fluorescent rhodamine derivatives. *Biophys. J.*, **76**; 469–477.

Savitskiy, V. P., Shman, T. V., Potapnev, M. P. 2003. Comparative measurement of spontaneous apoptosis in pediatric acute leukemia by different techniques. *Cytometry B Clin. Cytom.*, **56**; 16–22.

Sheik-Bahae, M., Said, A. A., Wei, T.-H., Hagan, D. J., Van Stryland, E. W., Sensitive measurement of optical nonlinearities using a single beam. 1990. *IEEE Journal of Quantum Electronics*, **26**; 760–769.

Smiley, S. T., Reers, M., Mottola-Harshorn, C., Lin, M., Smith, T. W., Steele, Jr. G. D., Chen, L. B. 1991. Intracellular heterogeneity in mitochondrial membrane potentials revealed by a J-aggregate-forming lipophilic cation JC-1. *Proc. Natl. Acad. Sci. USA*, **88**; 3671–3675.

So, P. T. C., Dong, C. Y., Masters, B. R., Berland, K. M. 2000. Two-photon excitation fluorescence microscopy. *Annu. Rev. Biomed. Eng.* **2**; 399–429.

Tani, S., Nakagawa, K., Honda, T., Saito, H., Suzuki, Y., Kawamata, J., Uchida, M., Sasaki, A., Kinjo, M. 2012. Fluorescence imaging of mitochondria in living cells using a novel fluorene derivative with a large two-photon absorption cross-section. *Current Pharmaceutical Biotechnology*, **13**; 2649–2654.

Wolleshensky, R., Feurer, T., Sauerbrey, R., Simon, U., Characterization and optimization of a laser-scanning microscope in the femtosecond regime. 1998. *Appl. Phys. B*, **67**; 87–94.

Table I. One- and two-photon optical properties of BP6 and FLW

Compound	λ_{abs} /nm [a]	λ_{fl} /nm [a]	α /10^{-29} m^3 [b]	$\sigma^{(2)}_{peak}$ /GM [c]
BP6	384	527	5.61	250
FLW	420	545	6.40	730

[a] λ_{abs} and λ_{fl} are the wavelengths of the absorption and one-photon fluorescence maximum, respectively. [b] α is the polarizability estimated by computational calculation. [c] $\sigma^{(2)}_{peak}$ is the maximum two-photon absorption cross-section.

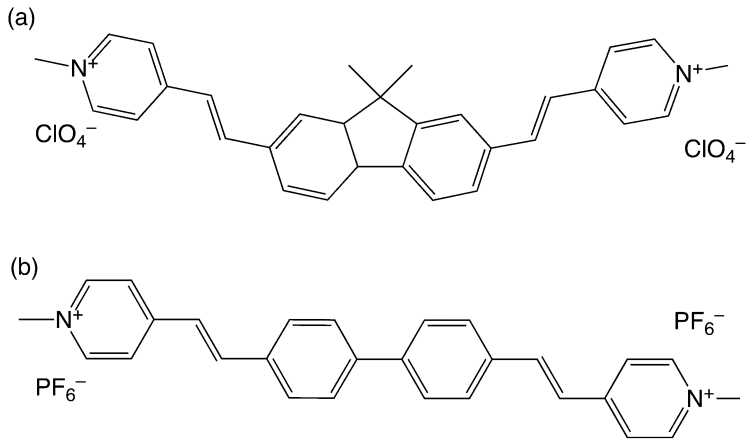

Fig. 1 Chemical structures of FLW (a) and BP6 (b)

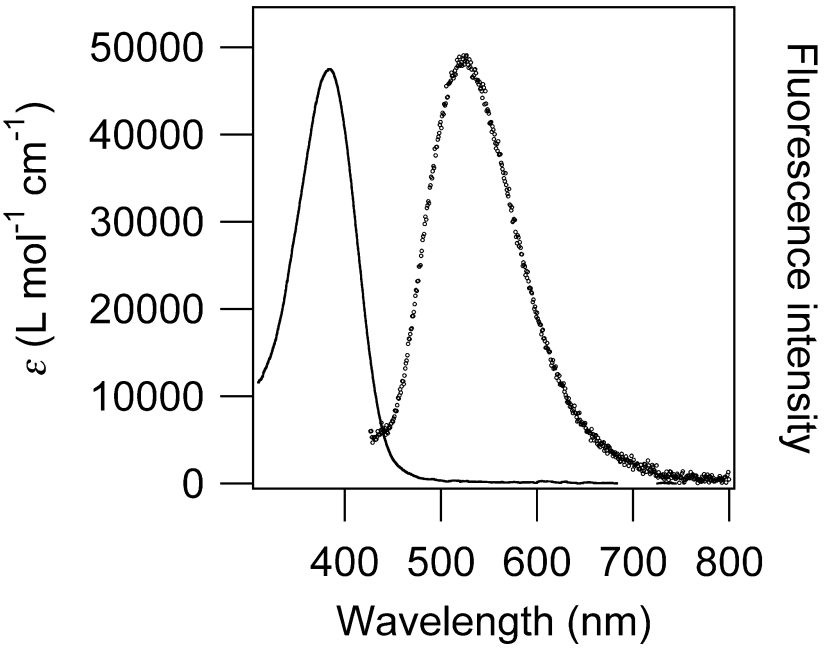

Fig. 2 Absorption (solid line) and fluorescence (dotted line) spectra of a 1 μM aqueous solution of BP6

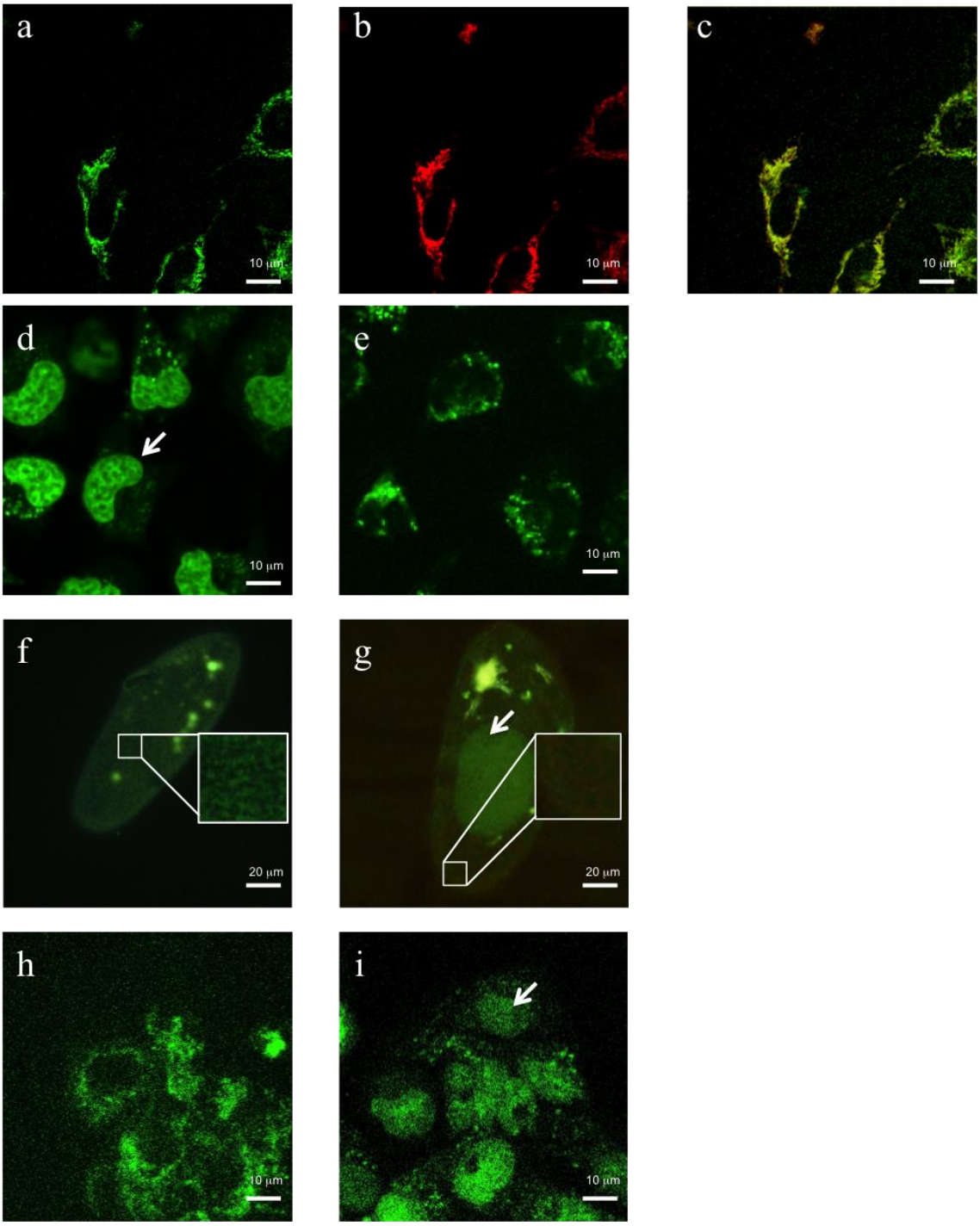

Fig. 3 Single photon fluorescence microscope (SPFM) images of HeLa cells, Hek293 cells, and *Paramecium caudatum* (*P. caudatum*). (a) shows HeLa cells stained with BP6. (b) shows HeLa cells stained with Mito Tracker. (c) is a merged image of (a) and (b). (d) and (e) show HeLa cells stained with BP6 after adding carbonyl cyanide

m-chlorophenyl hydrazine (CCCP) and after washing out and removing CCCP, respectively. SPFM images of *P. caudatum* before and after the addition of CCCP are shown in (f) and (g). Close-ups of the boxed areas are shown in the insets. Hek293 cells before and after the addition of CCCP are shown in (h) and (i). White arrows in (g) and (i) indicate the nucleus.

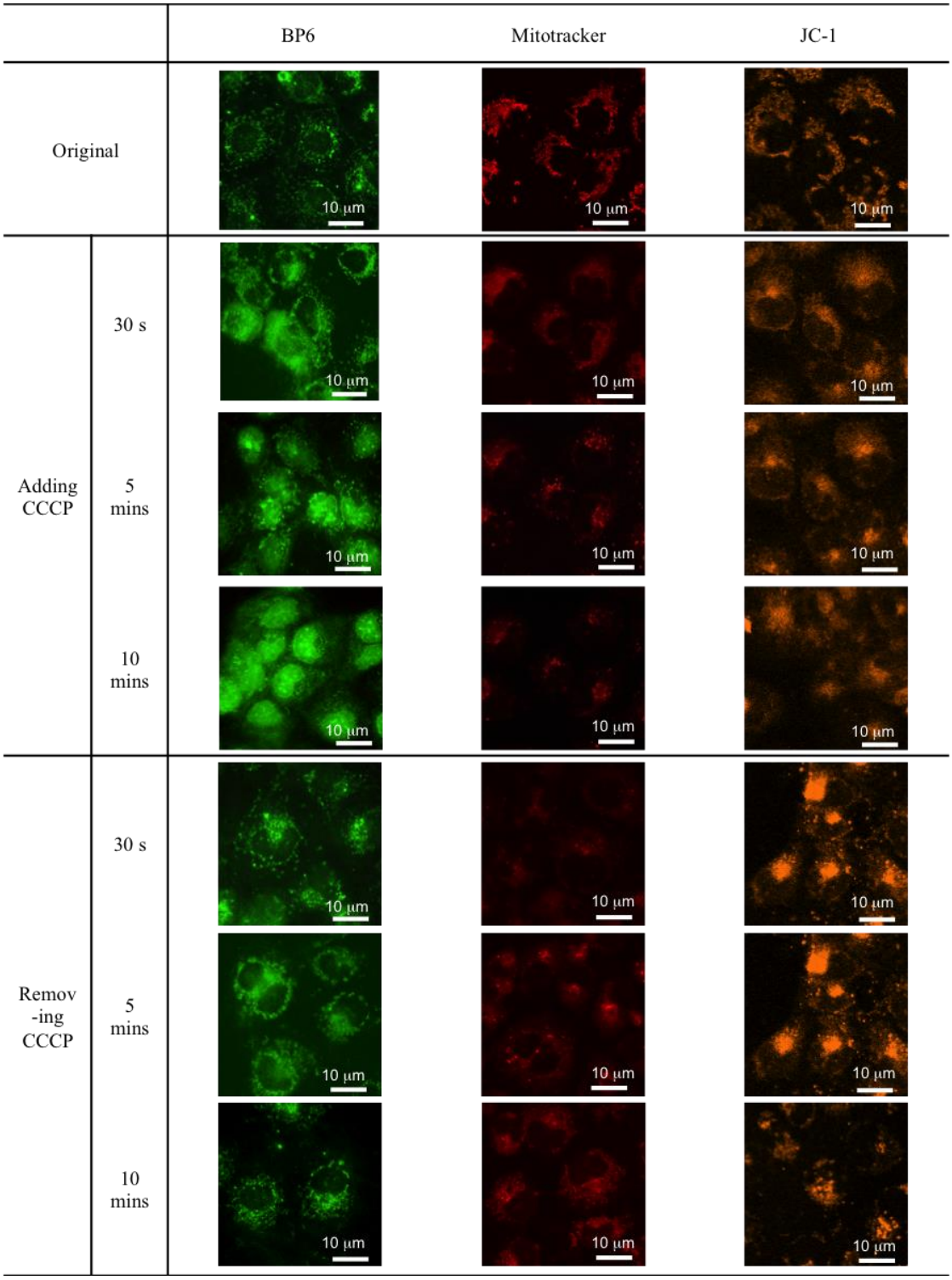

Fig. 4 Time-lapse SPFM images of Hek293 cells stained with BP6 (left), Mito Tracker (center) and JC-1 (right) before and after adding CCCP, and after removing the CCCP. Rows correspond to seconds or minutes after the addition or removal of CCCP. Cells

before the addition of CCCP are indicated as ‘Original’. Due to the difficulty of washing the cells while maintaining the field of view, the same cells were not always observed throughout the experiment.

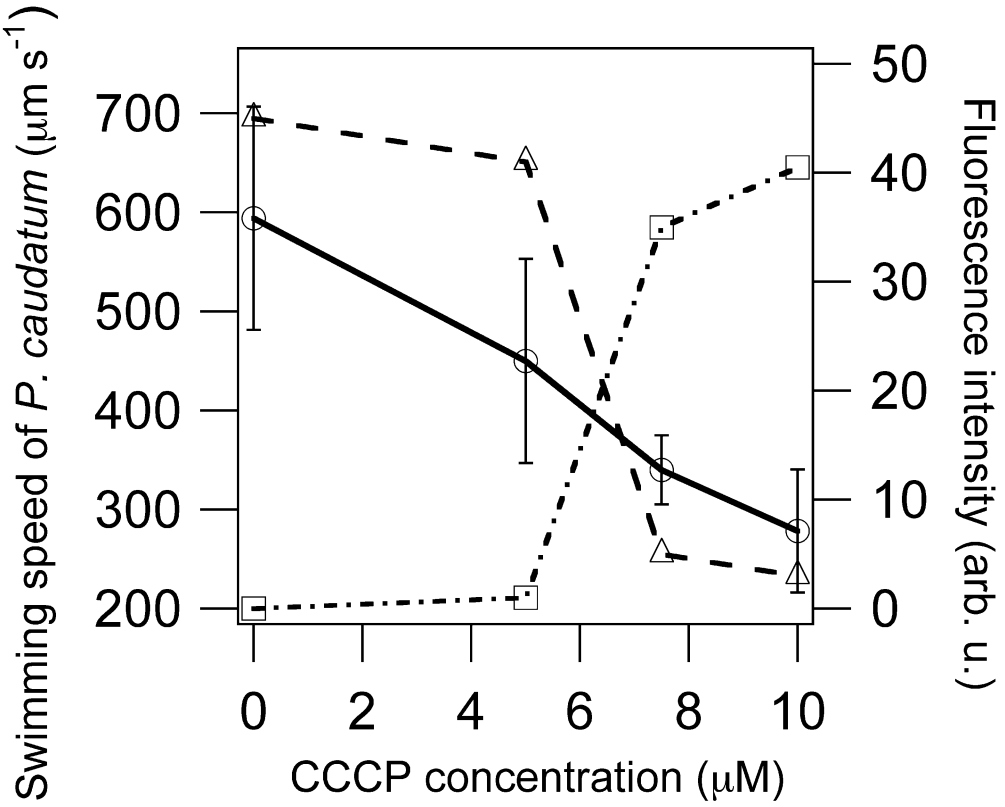

Fig. 5 Swimming speed of *P. caudatum* (○) and fluorescence intensity of the mitochondria (△) and the nucleus (□) versus CCCP concentration in the medium

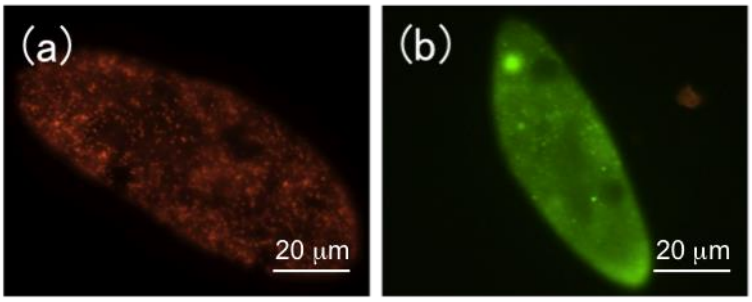

Fig. 6 SPFM image of *P. caudatum* stained with JC-1 in medium containing 5 μM (a) and 7 μM CCCP (b)

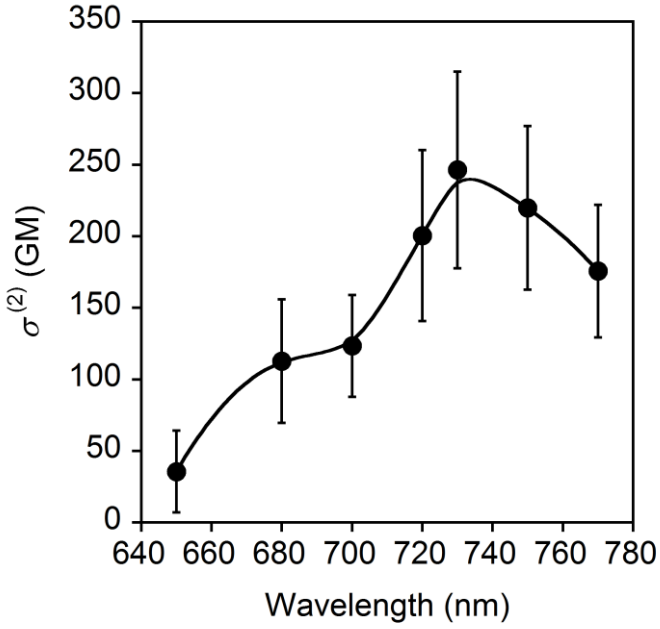

Fig. 7 Two-photon absorption spectrum of BP6 in 1 mM dimethylsulfoxide.

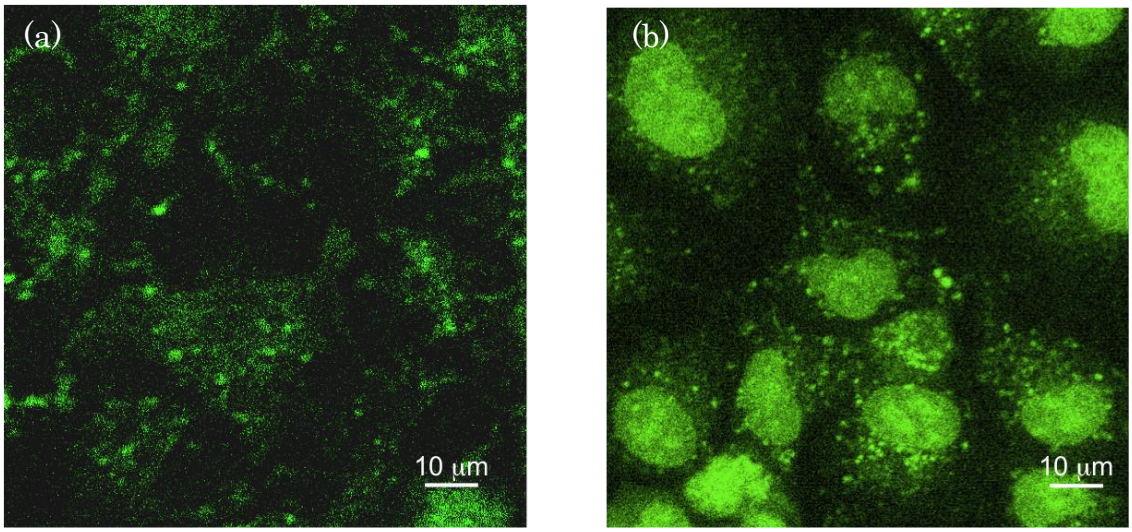

Fig. 8 Two-photon fluorescence microscope images of Hek293 cells before (a) and after (b) adding CCCP